Electrochemical Quantized Capacitance Charging of Surface Ensembles of Gold Nanoparticles

Shaowei Chen[†] and Royce W. Murray*

Kenan Laboratories of Chemistry, University of North Carolina, Chapel Hill, North Carolina 27599-3290

Received: July 29, 1999; In Final Form: September 9, 1999

Quantized double layer capacitance charging is observed for monolayers of nanometer-sized monolayer protected gold clusters (Au MPCs) anchored to macroscopic gold electrodes. The clusters were anchored in two ways. One method involves ligand place-exchange binding of an MPC covered with a butanethiolate monolayer to a preformed, self-assembled monolayer of 4,4′-thiobisbenzenethiol (TBBT) on Au. In the second method, an MPC with a mixed TBBT/heptanethiolate monolayer is prepared; this surface-reactive cluster anchors itself onto a gold electrode surface. Differential pulse voltammetry (DPV) of these MPC monolayers displays a succession of current peaks whose regular spacing on the potential axis is similar to that in DPV of solutions of the same, nonanchored MPCs. AC impedance measurements of the MPC monolayers show capacitance undulations that mirror the DPV results.

Introduction

The fabrication of nanometer-scale particles and arrays of particles and electrodes and the study of their electrical and electron-transfer properties are significant themes of current research.[1−3] In charging of nanoparticles by single electrons, the capacitance properties exhibited can be distinctive from those of particles with larger (≫ nanometer, "bulk") and smaller dimensions (molecular characteristics). For example, passage of a single electron at a 1 μm radius metal microdisk electrode immersed in a room-temperature electrolyte solution would evoke an unobservable sub-k_BT change (1.3 μV, assuming a 4 μF/cm^2 electrical double layer capacitance) in its rest potential. A readily observable change in rest potential (0.32 V) would, on the other hand, transpire for a one-electron transfer to (from) a 1.0 nm radius metal cluster dissolved in that solution.

Quantized (single electron) charging of nanoparticles has been observed in several ways. One experiment involves addressing[3,4] a single nanoparticle (which can range from ill-defined components of nanogranular structures to relatively well-defined, isolated metal nanoparticles where combinations of Au and organothiols have been popular) with a scanning tunneling microscope tip. In an electrochemical variant of this experiment, a nanometer-sized electrode was addressed with a redox-buffered electrolyte solution.[5] Large collections of nanoparticles also exhibit quantized charging, provided they are reasonably monodisperse ensembles. Quantized charging has been reported for transferred Langmuir trough arrays of monolayer-protected Ag clusters (Ag MPCs), sandwiched as Al/MPC array/polymer dielectric/Al devices,[6] and in electrochemical voltammetry in which dissolved Au MPCs diffused to a (macroscopic) electrode/solution interface.[7,8]

This paper demonstrates the electrochemical quantized charging of ensembles of nanoparticles that are chemically anchored at a macroscopic gold electrode/electrolyte solution interface. The nanoparticles are monolayer-protected Au clusters (Au MPCs) coated with monolayers of butanethiolate or heptanethiolate ligands. The linker molecule is 4,4′-thiobisbenzenethiol (TBBT). The quantized electrochemical charging is detected by the presence of current peaks in differential pulse voltammograms (DPV) and by capacitance peaks in ac impedance measurements. The monolayers are prepared by two different approaches, with similar results. The results are compared to those for the diffusion-controlled, quantized charging of dilute solutions of MPCs.

Experimental Section

Preparation of Clusters and Modified Surfaces. Monolayer-protected Au clusters (MPCs) were prepared by the Brust reaction.[9] Clusters prepared with butanethiolate monolayers (C4Au MPC) were supplied by Dr. T. G. Schaaff and Prof. R. L. Whetten (Georgia Institute of Technology) and had been fractionated[10] so as to isolate MPCs with monodisperse Au core sizes (1.6 nm dia.). The C4 MPCs had been characterized by ionization/desorption mass spectrometry to have core masses of 28 kDa and correspond, for an assumed truncated octahedral shape, to the formula ca. Au$_{145}$(C4)$_{50}$. The C4 MPCs were anchored by reaction (7 days, no change for longer exposures) of a ca. 0.1 mM toluene solution of MPC, with a self-assembled monolayer of 4,4′-thiobisbenzenethiol (TBBT, or [HS-p-Ph-]$_2$) on Au. The self-assembled monolayer was prepared by exposing a clean polycrystalline Au wire tip (0.017 cm^2, sealed in glass) to a 1 mM ethanol solution of TBBT for 24 h. The sequence of steps is shown in Figure 1A,C.

In a second procedure, MPCs with mixed monolayers of heptanethiolate and 4,4′-thiobisbenzenethiol (TBBT) (C7-TBBT-Au MPCs) were prepared by the Brust reaction,[9] by reacting a mixture of heptanethiol and TBBT (9:1 mole ratio) with chloroaurate (overall mole ratio of thiol to Au was 3:1) in toluene solution, followed by reduction using a 10-fold excess of borohydride. The isolated C7-TBBT-Au MPCs were ascertained to be free of excess reagents by proton NMR. The C7-TBBT-Au MPCs were used in both unfractionated and fractionated forms in comparative experiments. The C7-TBBT-Au MPCs were fractionated (partially) by precipitation from toluene

* Corresponding author e-mail: rwm@email.unc.edu.
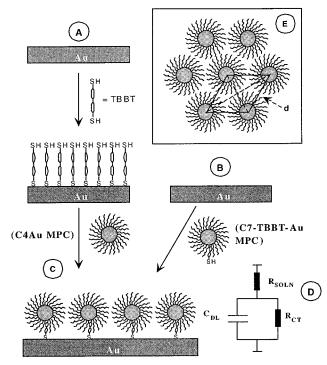† Present address: Department of Chemistry, Southern Illinois University, Carbondale, IL 62901-4409.

Electrochemical Quantized Capacitance Charging

J. Phys. Chem. B, Vol. 103, No. 45, 1999 **9997**

Figure 1. Cartoon reactions for anchoring MPCs to a Au electrode surface by two approaches: (A and C) reaction of a core-monodisperse butanethiolate-protected MPC (C4Au MPC), with a 4,4′-thiobisben-zenethiolate (TBBT) self-assembled monolayer on Au, and (B) reaction of a clean Au surface with an MPC with a mixed heptanethiolate/TBBT protecting monolayer (C7-TBBT-Au MPC, either unfractionated or partially fractionated). The anchored MPC monolayer in (C) shows only the linker TBBTs for simplicity; the other TBBT units are presumed to still be present. (D) shows the assumed electrochemical equivalent circuit of the modified Au interface, where R_{SOLN} is solution resistance, C_{DL} is electrode double layer capacitance, and R_{CT} is cluster/solution electron transfer resistance. (E) shows a schematic top view of anchored monolayer in which d is taken as average center−center core separation.

solution by addition of an equal volume of acetone. Following previous work,[10] the MPCs which did not precipitate from the more polar solvent mixture were smaller-core materials and were characterized by transmission electron microscopy (TEM) and preparation of histograms[7c,d] as having two major populations of Au core size: ca. 40% were 1.6 nm in diameter (ca. Au_{145}) and ca. 60% were 2.8 nm in diameter (avg. ca. Au_{807}). Combining results from TEM, NMR, and thermogravimetry as before[11] indicate an *overall average* monolayer composition of the partially fractionated MPC sample of ca. 92 C7 ligands and ca. 5 TBBT ligands per cluster. C7-TBBT-Au MPCs were anchored by reaction (Figure 1B) of a 0.1 mM toluene solution with a clean polycrystalline Au wire tip (0.17 cm^2) for 7 days.

The above procedures are not the only conceivable chemical pathways to immobilize MPCs. For example, Schiffrin et al.[12] have recently described the binding of "naked" Au clusters to a thiolated indium thin oxide electrode surface.

Electrochemical Measurements. Differential pulse voltammetry of MPC electrolyte solutions (0.1 mM MPC, in 0.05M Hx$_4$NClO$_4$ toluene:acetonitrile, 2:1 v:v, not degassed) was carried out using a BAS 100B electrochemical analyzer. The typical dc potential sweep rate was 10 mV/sec and the pulse amplitude 50 mV. AC impedance measurements (10 mV amplitude, 1 to 200 kHz) were conducted at a series of applied dc potentials using a Solartron Si 1287 electrochemical interface and a Solartron Si 1260 impedance/gain-phase analyzer. The partial semicircles produced by the frequency scans on the

impedance plots[13] were fitted using the instrument's software (ZPlot) to produce values of charge transfer resistance and double layer capacitance according to the equivalent circuit shown in Figure 1D.

Results and Discussion

The monolayers of MPCs were anchored to Au surfaces using the two approaches outlined in Figure 1. In one, a butanethiolate-protected cluster (C4Au MPC, with monodisperse[10] Au cores) is reacted (step C) with a thiol surface prepared by forming (step A) a self-assembled monolayer (SAM) on Au (i.e., the electrode) of the bifunctional thiol (4,4′-thiobisbenzenethiol, TBBT). The anchoring reaction (step C) was calculated to occur as a ligand place-exchange[14] in which one (or more) thiols on the TBBT SAM replace a butanethiolate ligand on the C4Au MPC. This reaction was successful, although quite slow.

The second approach relied on preparing a surface-reactive MPC by mixing in a small proportion of TBBT with heptanethiol in a Brust reaction procedure.[9] The mixed-monolayer MPC (C7-TBBT-Au MPC) was partially fractionated to decrease its core size dispersity. Anchoring of this surface-active MPC to a clean Au electrode surface is depicted in Figure 1, step B, and in principle produces an MPC monolayer linked to the Au surface in the same manner as that produced in steps A and C.

The heptanethiolate ligands were calculated to be of sufficient length as to sterically minimize TBBT-based coupling of MPCs with one another during the Brust reaction. The mixed monolayer C7-TBBT-Au MPCs are interesting materials, being isolable, reasonably stable, and soluble in a variety of organic solvents, unlike the aggregated products obtained[15] using *n*-alkanedithiols. Clusters that are stable and have built-in anchoring chemistry are uncommon and may have application to areas such as chemical sensors and catalysis.

The electrochemistry of the monolayers of anchored MPCs is shown in Figure 2. The topmost panels (Figure 2A,B) compare the differential pulse voltammetry (DPV) of the anchored MPCs to that of their solution counterparts. The DPV responses of toluene:acetonitrile solutions of C4Au and C7-TBBT-Au MPCs (Figure 2A,B (- - -), respectively) display well-defined, roughly evenly spaced, current peaks (which in Panel B are labeled with *). The spacing ΔV between adjacent single-electron charging peaks reflects the capacitance C_{CLU} (farads/cluster) of MPCs diffusing to the electrode through the simple relation $\Delta V = e/C_{CLU}$, where e is the electronic charge. The DPV responses for the MPCs anchored at the electrode/solution interface (Figure 2A,B −) also show roughly evenly spaced peaks. These peaks are smaller and less distinct than those of the diffusing MPCs, because the quantities of MPCs being electrochemically charged in the anchored monolayers are smaller, but on expanded scale diagrams they are readily seen as either peaks or inflections, well above background. The DPV of a Au surface that had been reacted with *unfractionated* C7-TBBT-MPCs is, in contrast, relatively featureless as shown in Figure 2B (···). In the unfractionated material, the polydispersity in cluster core size corresponds to a range of different cluster capacitances and consequent ΔV values; the overlap[8] of differently spaced peaks in the mixture obviates resolution of individual peaks.

Each successive current peak in Figure 2A,B corresponds to single electron chargings of MPCs that diffuse to the electrode or are anchored there. The displacements between the current peaks in positive- and negative-going dc potential scans are thought to be a trivial result of uncompensated solution resistance; averaging of those peak potentials gives a "formal
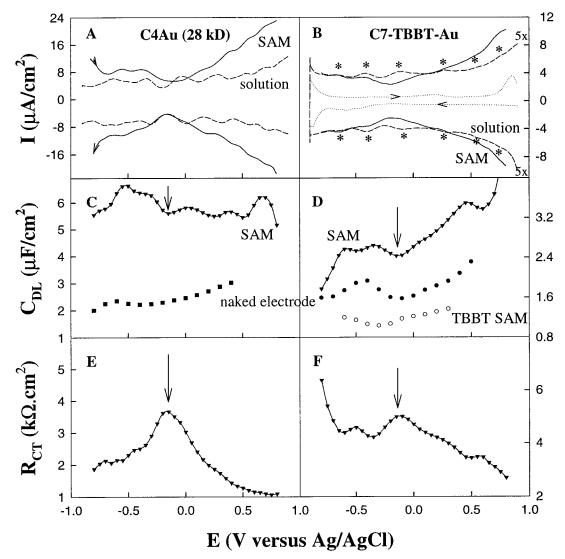
Figure 2. Differential pulse voltammograms (DPV, Panels A and B) and ac impedance-derived double-layer capacitances C_{DL} (Panels C and D) and charge transfer resistances R_{CT} (Panels E and F) of 0.1 mM MPC solutions (in 0.05 M Hx_4NClO_4 2:1 toluene:acetonitrile) and anchored MPCs. Left panels are based on preparations according to Figure 1A,C. Panel A: DPV of C4Au MPC solution (- - -) and anchored C4Au monolayer (—). Panel C: C_{DL} results for anchored C4Au monolayer (▼) and for TBBT monolayer self-assembled on Au (■). Panel E: R_{CT} results for anchored C4Au monolayer (▼). Right panels are based on preparations according to Figure 1B. Panel B: DPV of anchored monolayers of fractionated (—) and unfractionated (···) C7-TBBT-Au MPCs and solution of fractionated C7-TBBT-Au MPCs (- - -), for which the current peaks are labeled with an asterisk (*) and the experimental time of ca. 20 min is too short for surface attachment reaction of Figure 1B to be significant. Panel D: C_{DL} results for anchored monolayer of fractionated (▼) and unfractionated (○○○○) C7-TBBT-Au MPCs and naked Au electrode (•). Panel F: R_{CT} results for anchored, fractionated, C7-TBBT-Au MPC monolayer (▼). The sharp changes in C_{DL} and R_{CT} at the most negative potentials in panels D and F may be artifacts due to concurrent reduction of oxygen. E_{PZC} is thought to lie at the arrows in Panels C−F.

potential" that is characteristic of a certain change in the charge state (z) of the MPC core. The formal potentials for successive quantized double layer capacitance chargings, $z/z - 1$, can be shown[8] to vary with charge state as

$$E^0_{z,z-1} = E_{PZC} + \frac{(z - 1/2)e}{C_{CLU}} \qquad (1)$$

where E_{PZC} is the MPC potential of zero charge ($z = 0$), which is taken to be about −0.2 V versus Ag/AgCl according to the pronounced minima in the DPV traces (Figure 2A,B) and in the C_{DL} results from ac impedance (Figure 2C,D, see arrows). Double layer capacitance is well known to exhibit a minimum near the potential of zero charge of an electrified interface.[13] Equation 1 predicts linear plots of charging peak potentials ($E^0_{z,z-1}$) against charge state change. The charge state change $z = 0/+1$ is, for example, assigned to the first DPV peak that is positive of −0.2V (E_{PZC}). Such plots have been shown before[8]

for DPV results in MPC solutions and are given in Figure 3 for the Figure 2A,B results of solutions (Figure 3 ○, ▽) and anchored MPC monolayers (Figure 3 ●, ▼) of C4Au and C7-TBBT-Au MPCs. Except at the most positive charge states[17] of the C4Au MPCs, the plots are linear and have mostly similar slopes. The results for C_{CLU} for solution and anchored C4Au MPCs are 0.59 and 0.75 aF/cluster, respectively; for solution and anchored C7-TBBT-Au MPCs, the results are 0.55 and 0.53 aF/cluster, respectively. It is clear that MPCs have similar double layer capacitances whether dissolved in solution or surface anchored, i.e., surface anchoring has a minor effect on the nature of individual cluster/electrolyte solution interfaces.

Figure 2C−F (▼) shows results of ac impedance[13] measurements on the two kinds of anchored MPCs. In ac impedance, currents and their phase angles with applied voltage are measured as a function of ac potential frequency, the results being presented as impedances vectorially resolved into zero
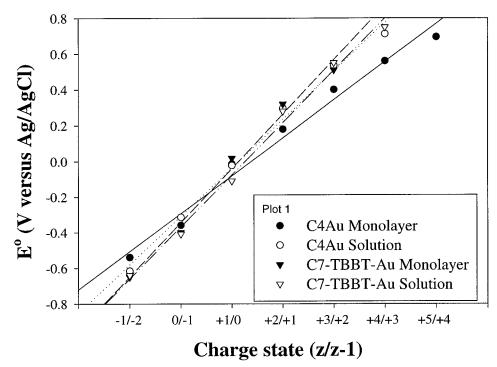
Electrochemical Quantized Capacitance Charging

J. Phys. Chem. B, Vol. 103, No. 45, 1999 **9999**

Figure 3. Plots of eq 1 for DPV formal potentials for C4Au and C7-TBBT-Au MPC solutions and anchored monolayers. Values of C_{CLU} from the slopes are 0.75 aF (C4 Au monolayer; 0.66 aF if the points in the curving, most positive potential part of the plot are omitted), 0.59 aF (C4 Au solution), 0.53 aF (C7-TBBT-Au monolayer), and 0.55 aF (C7-TBBT-Au solution). Calculation of C_{CLU} from the potential difference ΔV between the $z = +1/0$ and $0/-1$ DPV peaks gives 0.42 and 0.53 aF/cluster for solution C4 Au and C7-TBBT-Au MPCs, respectively, and 0.46 and 0.55 aF/cluster, respectively, for the anchored MPCs.

and 90° phase angle elements, which represent the resistive and capacitive characteristics, respectively, of the electrode/electrolyte interface. The capacitance and resistance results both show undulations, with maxima and minima. We next consider the origin of the undulations in capacitance and resistance and the significance of the individual values of resistance and capacitance. The results for capacitance will be considered first.

The maxima and minima of the undulations in capacitance in Figure 2C,D (▼) lie (within the resolution of the results) at the same potentials as the DPV current peaks in Figure 2A,B (−). It seems evident that the spacing between the capacitance undulations, as in DPV, manifests the spacing between the "formal potentials" (eq 1) of successive charge state changes of the ensembles of anchored MPCs. The capacitance undulations are formally analogous to redox pseudocapacitance peaks;[16,18] that is, the capacitance maximum at ca. +0.4 V in Figure 2D (▼) is a $z = 0/+1$ charging peak for removal of a single electron from each anchored C7-TBBT-Au cluster, which is formally analogous to the single electron oxidation of a ferrocene monolayer.

Other results in Figure 2C,D provide important supporting information. (a) The capacitances of a Au electrode bearing a TBBT monolayer (Figure 2C, ■) and of a naked Au electrode (Figure 2D, ●) are both smaller than that of surface-anchored MPC monolayers (Figure 2C,D, ▼). (b) The capacitance minimum for the TBBT monolayer (Figure 2C, ■) is shallow (as is typical of SAM surfaces[19]) and lies near −0.2 V, consistent with assignment of this value as the E_{PZC} of the MPC clusters. (c) Anchoring *unfractionated* C7-TBBT-Au MPCs (Figure 2D, ○) produces none of the charging peak fine structure seen for the fractionated MPC (Figure 2D, ▼), consistent with the analogous comparison in Figure 2B, and with simulations of effects of core size dispersity on the appearance of quantized charging responses of diffusing MPCs.[8]

The $z = 0/+1$ capacitance charging peaks in Figures 2C,D (▼) can be considered as parallel charging of a number of MPC capacitors equal to the coverage of surface-anchored MPCs. Assuming that the capacitances of individual surface-anchored C4Au and C7-TBBT-Au MPCs (i.e., 0.75 and 0.53 aF, from Figure 3) are the same as solution-dissolved ones yields estimates of their coverages of $8 \times 10^{12}/cm^2$ and $5 \times 10^{12}/cm^2$ (or 1.3×10^{-11} and 0.8×10^{-11} mol/cm²), respectively. These coverages correspond to average MPC footprint diameters of about 4 and 5 nm, respectively (assuming hexagonal close-packing, Figure 1E cartoon), dimensions which exceed the sum of actual average core diameters and monolayer chainlength and which imply that the monolayers are, on average, not tightly packed.

We turn last to interpretation of the resistance data in Figure 2E,F. Note that the undulations of the measured R_{CT} values seem to mirror those seen (Figure 2C,D) in capacitance, but with R_{CT} rising to maxima at potentials where C_{DL} drops to minima. Figure 1D presents an equivalent circuit of the electrode interface which contains a parallel resistance/capacitor combination (which is measured in Figures C−F) in series with the uncompensated solution resistance (the latter is eliminated during the impedance analysis). The observed parallel $R_{CT}C_{DL}$ equivalent circuit could be one of two possible combinations. In one, the R_{CT} charge transfer resistance element could represent the resistance, $R_{CT,LINK}$, of the 4,4′-thiobisbenzenethiolate linker molecule(s) between the electrode and MPC, and C_{DL} represents the capacitance $C_{DL,EL}$ of the electrode/MPC interface. In the second possibility, the C_{DL} term represents the double layer capacitance of the anchored MPCs (C_{CLU}, measured above) in their electrolyte bath, and R_{CT} represents the resistance to charge transfer ($R_{CT,MPC}$) of the MPC interface with the solution, or with surrounding MPCs. We will conclude, below, that the resistance element of the latter RC combination is probably that which is detected in Figure 2E,F.

Consider the capacitance elements of the two above possibilities. A capacitance $C_{DL,EL}$ can be reasonably assumed to be very small, on the basis of the (above-noted) similarity of spacing of the capacitance charging peaks for the anchored MPCs to those of solution-dissolved MPCs. On the other hand, assuming that the measured C_{DL} is instead the double layer capacitance of MPCs in the anchored monolayer is consistent with the Figure 3 analysis of the capacitance undulations in Figure 2. Additionally, if a significant population of electrolyte ions could squeeze between the electrode and the layer of anchored MPCs, the ensuing screening of the electrostatic interaction between electrode and MPC would shift the apparent "formal potentials" of the MPC charging steps, in an effect analogous to that for redox monolayers discussed by Smith and White.[20]

Considering next the charge transfer resistances measured in Figure 2E,F, they are more likely to reflect values of $R_{CT,MPC}$ than $R_{CT,LINK}$. This assignment can be made from the following three arguments. First, a calculation of the electron transfer rate constant (k_{LINK}) between electrode and MPC (i.e., a Au–linker–Au electron transfer), assuming that the measured R_{CT} is actually $R_{CT,LINK}$, gives $k_{LINK} = 10$ s^{-1} (for $R_{CT} = 2.5 \times 10^3$ Ω, at the $z = 0/+1$ potential in Figure 2E). This rate constant seems much too small when related data are considered. For example, the rate constant[21,22] for oxidation of ferrocene linked to Au through a well-ordered hexanethiolate linker (the same number of intervening carbons as the TBBT linker) is 2.5×10^5 s^{-1}, or over 10^4 times larger. Such a large difference seems unlikely, even allowing for electronic uncoupling incurred by twisting of the phenyl rings in the 4,4′-thiobisbenzenethiol linker molecule. Second, calculation of the effective resistance of an individual TBBT linker molecule, based on $R_{CT} = 2.5 \times 10^3$ Ω and 8×10^{12}/cm^2 coverage, gives 2×10^{16} Ω/molecule. This value is much larger than the $0.9-2 \times 10^7$ Ω/molecule values reported for the resistance of another (shorter) linker molecule, 1,4-dithiobenzene, from STM[3,6] and break junction[23] experiments. Third, were $R_{CT,MPC} \ll R_{CT,LINK}$, the groups of MPCs short-circuited together by electron transfers between MPCs (*laterally* within the monolayer) would, owing to the collectively larger capacitance, exhibit a decreased spacing (relative to dissolved MPCs) between the single electron charging peaks; this is not seen. Thus, while the value of $R_{CT,LINK}$ is the more interesting item in the Figure 1D equivalent circuit, and assuming the molecular resistance results[3,6,23] are correct, we believe that the measured R_{CT} is not that resistance element.

It is difficult to be certain whether the resistance $R_{CT} = R_{CT,MPC}$ represents electron transfer laterally between MPCs in the monolayer or between the MPC monolayer and parasitic impurities in the solution. In either case, one can argue that the undulations in the R_{CT} resistance measurements are *indirectly* caused by those in capacitance. Note that as the Au electrode potential is varied linearly, the potential at the MPC/electrolyte plane does not increase in a similarly linear manner, but "jumps" as successive quantized charging steps occur. Such potential jumps would effect apparent decreases in charge transfer resistance.

It can be seen that the ac impedance measurements allowed a somewhat closer scrutiny of the behavior of anchored MPC monolayers, relative to the DPV experiment, but even then some uncertainties remain regarding the detailed nature of the equivalent circuit. Nonetheless, the methodologies presented here may have value in the fabrication of long-range supramolecular nanoarchitectures. There is also basic significance in the possibility of study of interfacial electron transfer kinetics,[21,22] of novel molecular junctions, and of the interrelation of charging properties and functional labeling of the MPC surface.[24]

References and Notes

(1) See reviews: (a) Ulman, A. *An Introduction to Ultrathin Organic Films, From Langmuir–Blodgett to Self-Assembly*; Academic Press: Boston, 1991. (b) Schmid, G. *Clusters and Colloids: From Theory to Applications*; VCH: New York, 1994. (c) Grabert, H.; Devoret, M. H. *Single-Charge Tunneling*, Plenum: New York, 1992.

(2) For example: (a) Whitesides, G. M.; Mathias, J. P.; Seto, C. T. *Science* **1991**, *254*, 1312. (b) Stupp, S. I.; Lebonheur, V.; Walker, K.; Li, L. S.; Huggins, K. E.; Keser, M.; Amstutz, A. *Science* **1997**, *276*, 384. (c) Freeman, R. G.; Brabar, K. D.; Allison, K. J.; Bright, R. M.; Davis, J. A.; Guthrie, A. P.; Hommer, M. B.; Jackson, M. A.; Smith, P. C.; Walter, D. G.; Natan, M. J. *Science* **1995,** *267*, 1629. (d) Brabar, K. C.; Smith, P. C.; Musick, M. D.; Davis, J. A.; Walter, D. G.; Jackson, M. A.; Buthrie, A. P.; Natan, M. J. *J. Am. Chem. Soc.* **1996**, *118*, 1148. (e) Peschel, S.; Schmid, G. *Angew. Chem. Int. Ed. Engl.* **1995**, *34*, 1442. (e) Schmid, G.; Peschel, S.; Sawitowski, T. *Anorg. Allg. Chem.* **1997,** *623*, 719. (f) Feldheim, D. L.; Keating, C. D. *Chem. Soc. Rev.* **1998**, 27, 1.

(3) (a) Andres, R. P.; Bein, T.; Dorogi, M.; Feng, S.; Henderson, J. I.; Kubiak, C. P.; Mahoney, W.; Osifchin, R. G.; Reifenberger, R. *Science* **1996**, *272*, 1323. (b) Dorogi, M.; Gomez, J.; Osifchin, R.; Andres, R. P.; Reifenberger, R. *Phys. Rev. B* **1995**, *52*, 9071. (c) Andres, R. P.; Bielefeld, J. D.; Henderson, J. I.; Janes, D. B.; Kolagunta, V. R.; Kubiak, C. P.; Mahoney, W. J.; Osifchin, R. G. *Science* **1996**, *273*, 1690.

(4) (a) Hartmann, E.; Marquardt, P.; Ditterich, J.; Radojkovic, P.; Steinberger, H. *Appl. Surf. Sci.* **1996**, *107*, 197. (b) Sato, T.; Ahmed, H. *Appl. Phys. Lett.* **1997**, *70*, 2759. (c) Guo, L.; Leobandung, E.; Chou, S. Y. *Science* **1997**, *275*, 649. (d) Amman, M.; Wilkins, R.; Ben-Jacob, E.; Maker, P. D.; Jaklevic, R. C. *Phys. Rev. B* **1991**, *43*, 1146. (e) Hofstetter, W.; Zwerger, W. *Phys. Rev. Lett.* **1997**, *78*, 3737.

(5) Fan, R.-F. F.; Bard, A. J. *Science* **1997**, *277*, 1791.

(6) Markovich, G.; Leff, D. V.; Chung, S. W.; Soyez, H. M.; Dunn, B.; Heath, J. R. *Appl. Phys. Lett.* **1997**, *70*, 3107.

(7) (a) Ingram, R. S.; Hostetler, M. J.; Murray, R. W.; Schaaff, T. G.; Khoury, J. T.; Whetten, R. L.; Bigioni, T. P.; Guthrie, D. K.; First, P. N. *J. Am. Chem. Soc.* **1997**, *119*, 9279. (b) Chen, S.; Ingram, R. S.; Hostetler, M. J.; Pietron, J. J.; Murray, R. W.; Schaaff, T. G.; Khoury, J. T.; Alvarez, M. M.; Whetten, R. L. *Science* **1998**, *280*, 2098. (c) Chen, S.; Murray, R. W. *Langmuir* **1999**, *15*, 682. (d) Hicks, J. F.; Templeton, A. C.; Chen, S.; Sheran, K. M.; Jasti, R.; Murray, R. W. *Anal. Chem.* **1999**, *71*, 3703–3711.

(8) Chen, S.; Murray, R. W.; Feldberg, S. W. *J. Phys. Chem. B* **1998**, *102*, 9898.

(9) Brust, M.; Walker, M.; Bethell, D.; Schiffrin, D. J.; Whyman, R. *J. Chem. Soc., Chem. Commun.* **1994**, 801.

(10) Schaaff, T. G.; Shafigullin, M. N.; Khoury, J. T.; Vezmar, I.; Whetten, R. L.; Cullen, W. G.; First, P. N.; Gutierrezwing, C.; Ascensio, J.; Jose-Yacaman, M. J. *J. Phys. Chem. B* **1997**, *191*, 7885.

(11) Hostetler, M. J.; Wingate, J. E.; Zhong, C.-J.; Harris, J. E.; Vachet, R. W.; Clark, M. R.; Londono, J. D.; Green, S. J.; Stokes, J. J.; Wignall, G. D.; Glish, G. L.; Porter, M. D.; Evans, N. D.; Murray, R. W. *Langmuir* **1998**, *14*, 17.

(12) Baum, T.; Bethell, D.; Brust, M.; Schiffrin, D. J. *Langmuir* **1999**, *15*, 866.

(13) Bard, A. J.; Faulkner, L. R. *Electrochemical Methods*; Wiley: New York, 1980.

(14) (a) Hostetler, M. J.; Green, S. J.; Stokes, J. J.; Murray, R. W. *J. Am. Chem. Soc.* **1996**, *118*, 4212. (b) Hostetler, M. J.; Templeton, A. C.; Murray, R. W. *Langmuir* **1999**, *15*, 3782.

(15) Brust, M.; Bethell, D.; Schiffrin, D. J.; Kiely, C. J. *Adv. Mater.* **1995**, *7*, 795.

(16) Weaver, M. J.; Gao, X. *J. Phys. Chem.* **1993**, *97*, 332.

(17) The curvature at the most positive potentials in Figure 3 corresponds to an increase in capacitance there and probably reflects ion penetration into the monolayer.[7d]

(18) Chidsey, C. E. D.; Murray, R. W. *J. Phys. Chem.* **1976**, *90*, 1479.

(19) Becka, A. M.; Miller, C. J. *J. Phys. Chem.* **1993**, *97*, 6233.

(20) Smith, C. P.; White, H. S. *Anal. Chem.* **1992**, *64*, 2398.

(21) Smalley, J. F.; Feldberg, S. W.; Chidsey, C. E. D.; Linford, M. R.; Newton, M. D.; Liu, Y. P. *J. Phys. Chem.* **1995**, *99*, 13141.

(22) Chidsey, C. E. D. *Science* **1991**, *251*, 919.

(23) Reed, M. A.; Zhou, C. Muller, C. J.; Burgin, T. P.; Tour, J. M. *Science* **1997**, *278*, 252.

(24) Templeton, A. C.; Hostetler, M. J.; Warmoth, E. K.; Chen. S.; Hartshorn, C. M.; Krishnamurthy, V. M.; Forbes, M. D. E.; Murray, R. W. *J. Am. Chem. Soc.* **1998**, *120*, 4845.